Report no. changed (Mar 2006): SR-245-UU

SACLANTCEN REPORT
serial no: SR-245

SACLANT UNDERSEA RESEARCH CENTRE REPORT

ON THE PREDICTABILITY OF SUBSURFACE SOUND SPEED FROM SATELLITE-MEASURED SEA-SURFACE TEMPERATURE IN THE MEDITERRANEAN

H.H. Essen

January 1996

Report no. changed (Mar 2006): SR-245-UU

SACLANT Undersea Research Centre
Viale San Bartolomeo 400
19138 San Bartolomeo (SP), Italy

tel: +39-187-540.111
fax: +39-187-524.600

e-mail: library@saclantc.nato.int

NORTH ATLANTIC TREATY ORGANIZATION

On the predictability of subsurface sound speed from satellite-measured sea-surface temperature in the Mediterranean

H.-H. Essen

The content of this document pertains to work performed under Project 23 of the SACLANTCEN Programme of Work. The document has been approved for release by The Director, SACLANTCEN.

Director

intentionally blank page

On the predictability of subsurface sound speed from satellite-measured sea-surface temperature in the Mediterranean

H.-H. Essen

Executive Summary: In recent years the rapid assessment of unknown areas has become one of the main research tasks at SACLANTCEN for which satellite remote sensing is an appropriate tool. Satellite sensed data map large areas of the ocean and are (for some sensors) available in nearly real-time. The disadvantage is that the information is limited to parameters such as: ocean colour, sea-surface temperature, sea-surface roughness, and sea-surface topography. For sonar performance prediction, information on the boundaries, sea surface and seafloor, is required and for the inner ocean, the variability of sound speed.

In the Iceland-Faroe Frontal (IFF) area it has been found that (to some extent) subsurface sound-speed may be determined from satellite measured sea-surface temperatures (SST). The basic ideas behind the method are: Sound-speed profiles can be well represented by superposition of a small number of what are now referred to as Empirical Orthogonal Eigenfunctions (EOF), and the amplitudes of these EOFs are significantly correlated with SST.

This report applies this method to different areas in the Mediterranean Sea. The *in-situ* data needed, i.e. the sound-speed, have been determined by hydrographic (CTD) surveys, carried out on NRV *Alliance*. The SST images are from the Advanced Very High Resolution Radiometer (AVHRR) of the series of the NOAA polar-orbiting satellites, partly purchased from the University of Dundee (UK) or acquired by the new high-resolution satellite-receiver (*TeraScan*) of SACLANTCEN.

Tests have indicated that the method generally requires spatial variation of SST which exceed the accuracy of satellite-retrieved values ($\pm 0.5°C$). In addition, the water-mass structure should allow the vertical sound-speed profiles to be relatively smooth. These conditions have been fulfilled only for one of four surveys, in the area south of Sicily. Here, the 1st EOF accounts for the major part of the sound-speed variance and contains important information on its variability, mainly on long scales. The amplitude of the 1st EOF is highly correlated with SST and may be determined from satellite data.

intentionally blank page

On the predictability of subsurface sound speed from satellite-measured sea-surface temperature in the Mediterranean

H.-H. Essen

Abstract: The report investigates the extent to which subsurface sound speed may be determined from satellite-measured sea-surface temperature (SST). Using CTD data from four hydrographic surveys in the Mediterranean, it is shown that the vertical sound-speed profiles can be decomposed into Empirical Orthogonal Eigenfunctions (EOF), with the first three functions accounting for at least 88% of the variance. Significant correlation between EOF amplitudes and SST has been found for only one of the three EOFs, either the 1st EOF or the 2nd EOF. In order to determine subsurface sound-speed from SST, this EOF has to represent important features of the sound-speed variability. This is the case for only one of the four surveys. Failures for the other surveys are due to a combination of low spatial variability of SST, not visible in the satellite-retrieved values, and complex vertical sound-speed profiles, which may not be represented by one EOF only.

Keywords: Mediterranean coastal waters – satellite imagery – sea-surface temperature – sound-speed profiles

Contents

Acknowledgements: The author is grateful to the crews of the NATO research vessel *Alliance* and the Italian Navy Research vessel *Ammiraglio Magnaghi*. The CTD data were collected and processed by the Ocean Engineering Department (OED) and Large Scale Acoustics and Oceanographic Group (LSG) at SACLANTCEN. E. Nacini from SACLANTCEN processed the AVHRR images.

1 Introduction

Hydrographic surveys take some time and the spatial information may be distorted by temporal variability. One advantage of satellite remote sensing is the quasi-synoptic mapping, e.g. of sea-surface temperature (SST). Unfortunately, satellite measurements are restricted to the sea surface and provide no direct subsurface information, which is needed for the prediction of sonar performance.

Since 1978 SST has been measured from the NOAA series of polar-orbiting satellites by means of the Advanced Very High Resolution Radiometer (AVHRR). Recently, SACLANTCEN has purchased a high-resolution receiving system, which is operated either from the NATO Research Vessel (NRV) *Alliance* or from the Centre. The optimum resolution is 1.1 km, and the system allows mapping of the entire Mediterranean, currently the main research area of the Centre. With two satellites in orbit, the swath of about 3000 km yields global coverage four times a day. However, the requirement of a cloud-free sky for SST retrieval may considerably reduce the number of usable images.

From the Gulf Stream area it is known that temperature as function of depth, and in turn, sound speed can be well represented by a small number of Empirical Orthogonal Eigenfunctions (EOF), cf. Carnes *et al.* [1]. This holds also for the Iceland-Faeroe Frontal (IFF) area, as Essen and Sellschopp [2] showed by making use of CTD and thermistor chain data. For both areas, high correlation exists between the 1st- and 2nd-order EOF amplitudes with dynamic height at the sea surface. In the IFF area, dynamic height may not be measured from space with the accuracy needed. For this reason, Essen and Sellschopp [2] investigated the correlation between EOF amplitudes and SST. They found a high correlation between SST and the amplitude of the 1st EOF, which contains important information mainly on the long-scale variability of the subsurface sound speed.

The present investigations make use of CTD data gathered during four cruises of NRV *Alliance* in the Mediterranean. All data are from coastal areas, south of the islands Elba and Sicily and from the Otranto Gap. For retrieving features of subsurface sound-speed from satellite-measured SST, the variability of SST should exceed the accuracy of the satellite data. In addition, the water-mass structure should allow the vertical sound-speed profiles to be relatively smooth. These conditions have been fulfilled only for one of four surveys, in the area south of Sicily. Here,

the 1st EOF accounts for the major part of the sound-speed variance and contains important information on its variability. The amplitude of the 1st EOF is highly correlated with SST and may be determined from satellite data.

2

Method of analysis

The analysis presented here consists of three steps. The first step is the decomposition of the sound-speed profiles into a limited number of EOFs and the determination of the EOF amplitudes of each profile. Then these amplitudes are compared with the SST, i.e. the temperature of the uppermost layer of the CTD cast. This relation is quantified by means of a regression analysis. Finally, SSTs are collected from a satellite image along a chosen section. EOF amplitudes are determined *via* the regression curves and sound-speed profiles are reconstructed by means of the EOFs.

2.1 EOF-analysis

The deviation from the mean sound-speed profile may be decomposed into EOFs by,

$$c_{ln} = \sum_{m=1}^{M} a_n^{(m)} e_l^{(m)} \quad with, \quad c_{ln} = C_{ln} - C_{l0}, \quad C_{l0} = 1/N \sum_{n=1}^{N} C_{ln}. \tag{1}$$

C_{ln} are the sound-speed profiles at locations $n = 1, ..., N$, with $l = 1, ..., L$ counting their depth horizons. C_{l0} is the mean sound speed at depth l. The $e_l^{(m)}$ are the mutually orthogonal EOFs of order $m = 1, ..., M \leq L$, determined by the eigenvalue problem,

$$\sum_{k=1}^{L} R_{lk} e_k^{(m)} = \lambda^{(m)} e_l^{(m)} \quad with, \quad R_{lk} = 1/N \sum_{n=1}^{N} c_{ln} c_{kn}, \tag{2}$$

where R_{lk} is the covariance matrix of the data. The eigenvalues $\lambda^{(m)}$ describe the amount of variance as explained by the respective mode. Normally, a small number of modes contains most of the variance and summation over m in (1) may be restricted to values M considerably smaller than L. The mode amplitudes $a_n^{(m)}$ in (1) are given by,

$$a_n^{(m)} = \sum_{l=1}^{L} c_{ln} e_l^{(m)}, \tag{3}$$

and determine the sound-speed profile at position n.

2.2 Regression analysis

In order to quantify the dependence of EOF amplitudes on SST, a regression analysis is performed. The EOF amplitudes a_n, as defined by (3), are approximated through a polynomial of order K, of which the coefficients γ_k are determined by a least-squares fit,

$$\epsilon^2 = \sum_{n=1}^{N} [a_n - (\gamma_o + \sum_{k=1}^{K} \gamma_k T_n^k)]^2 = \textit{minimum}, \tag{4}$$

where T_n is the SST at position n. This fit is performed for each significant EOF mode separately. The quality of the approximation may be described by the coefficient,

$$r^2 = \frac{s^2 - \epsilon^2}{s^2}, \tag{5}$$

where s^2 is the variance of the amplitudes a_n. In the case of a linear dependence, i.e. $K = 1$ in (4), r is the correlation coefficient.

3 Data

In this report we analyse sound-speed profiles from four cruises of NRV *Alliance* to different areas of the Mediterranean. The sound speed profiles have been deduced from measurements with MK-III CTD systems. Pressure, temperature and conductivity are acquired during the downcasts with a sampling frequency of 25 Hz, while the system is lowered at about 1 ms^{-1}. Casts are usually taken down to within some 10 m of the bottom. Sound speed is computed from the CTD data using formulation from Brekhovskikh and Lysanov [3],

$$c = 1449.2 + 4.6T - 0.055T^2 + 0.00029T^3 + (1.34 - 0.01T)(S - 35) + 0.016D, \quad (6)$$

where c [ms^{-1}] is the sound speed, T [°C] the temperature, S [ppt] the salinity and D [m] the depth. For the EOF analysis, sound-speed has been averaged within vertical layers of 5 m, centered at 3 m, 8 m, etc.

During an acoustic experiment south of Elba, CTD casts were made from 27 August to 9 September 1994 (14 days), over a very limited area. From 13 to 22 November 1994 (10 days), a hydrographic survey was carried out south of Sicily. Another data set from south of Elba was gathered from 21 April to 2 May 1995 (12 days), over a more extended area. The last data set is from the Otranto Gap. The hydrographic measurements of NRV *Alliance* were supported by the Italian Navy Research Vessel (IRV) *Ammiraglio Magnaghi*. A quasi-synoptic survey of the Otranto Gap was completed in less than 5 days, from 19 to 23 May 1995. Times and positions of all CTD casts used for the following analysis are listed in Annex A.

During the experiments, surface meteorological data and sea-surface temperature were recorded with the ZENO-Alliance network (ZAN), ZENO and ZAN being trade names of the Coastal Climate Company (Seattle, USA). ZAN is a monitoring system designed specially for shipboard installation, cf. Minnett [4]. The network integrates measurements of apparent wind, air temperature, relative humidity, barometric pressure and water temperature with information on ship location, course and heading. Wind is measured on the foremast at about 16 m above the water line, and water temperature at about 2 m below sea surface on the port side of NRV *Alliance* (2.5 m above her keel). For the periods of the hydrographic measurements, time series of air- and water temperature, relative humidity and wind speed are displayed in Annex B.

The Advanced Very High Resolution Radiometer (AVHRR), in the NOAA series of polar-orbiting weather satellites, is a five-channel device, two channels viewing the visible and three the infrared. Visible data values may be converted to albedos, and infrared channels into brightness temperature. The infrared channels are in so-called atmospheric windows where the atmosphere is relatively transparent. Due to atmospheric effects the brightness temperature does not correspond to the SST. In general, the brightness temperature underestimates the SST.

Only the infrared channel-4 is used, centered at 10.8 μm. In order to account for the deviation from SST, we determine the difference between measured SST and channel-4 brightness temperature at the position of NRV *Alliance*, and use it for correction.

4

Data analysis

The data analysed are from four hydrographic surveys carried out by NRV *Alliance* in the Mediterranean. Two of them supported acoustic tomographic experiments south of Elba. The other two were performed for oceanographic investigations south of Sicily and in the Strait of Otranto. In order to obtain a quasi-synoptic view a second ship was used for the latter survey.

4.1 Elba (Aug/Sep-94)

The upper part of Fig. 1 shows the channel-4 brightness temperatures of the AVHRR of NOAA-11 on 28 August 1994. This is the first of 11 days from which CTD casts have been chosen for analysis. The position of NRV *Alliance* during the satellite overpass is marked by a cross. It is just in a strong gradient of SST. While the brightness temperature changes from 23.8°C to 23.1°C between two adjacent pixels the ship-borne measurement shows a decrease from 26.9°C to 26.0°C within 10 min. The brightness temperature underestimates the SST by about 2.9°C. For the following analysis, we add this difference to the brightness temperature and refer to the result as SST.

While the CTD surveys of the other experiments extend over a large area, the CTD profiles of the Elba-94 experiment are from approximately the same position. Out of 189 profiles 38 have been selected for EOF analysis. These profiles are from a restricted area of about 10 km in diameter, they all extend to 100 m depth and are separated by at least 1 h in time. The locations are displayed in the lower part of Fig. 1. Measuring times and positions are listed in Table A1 of Annex A. Most of the data are separated by only 1 h, but between the phases of extensive CTD activities there are gaps of a few days. All the CTD casts were taken during day time.

The sound-speed data of each profile have been averaged into 20 depth intervals of 5 m extension centered at 3, 8,..., 98 m. Figure 2 (left panel) displays the profiles (dotted lines). The first three (arbitrarily normalised) EOFs are presented and the degree of variance is indicated. This is 84% for the 1st EOF and 94% for 1st to 3rd EOF. It is concluded that the measured sound-speed profiles may be reasonably represented by the superimposition of the first three EOFs.

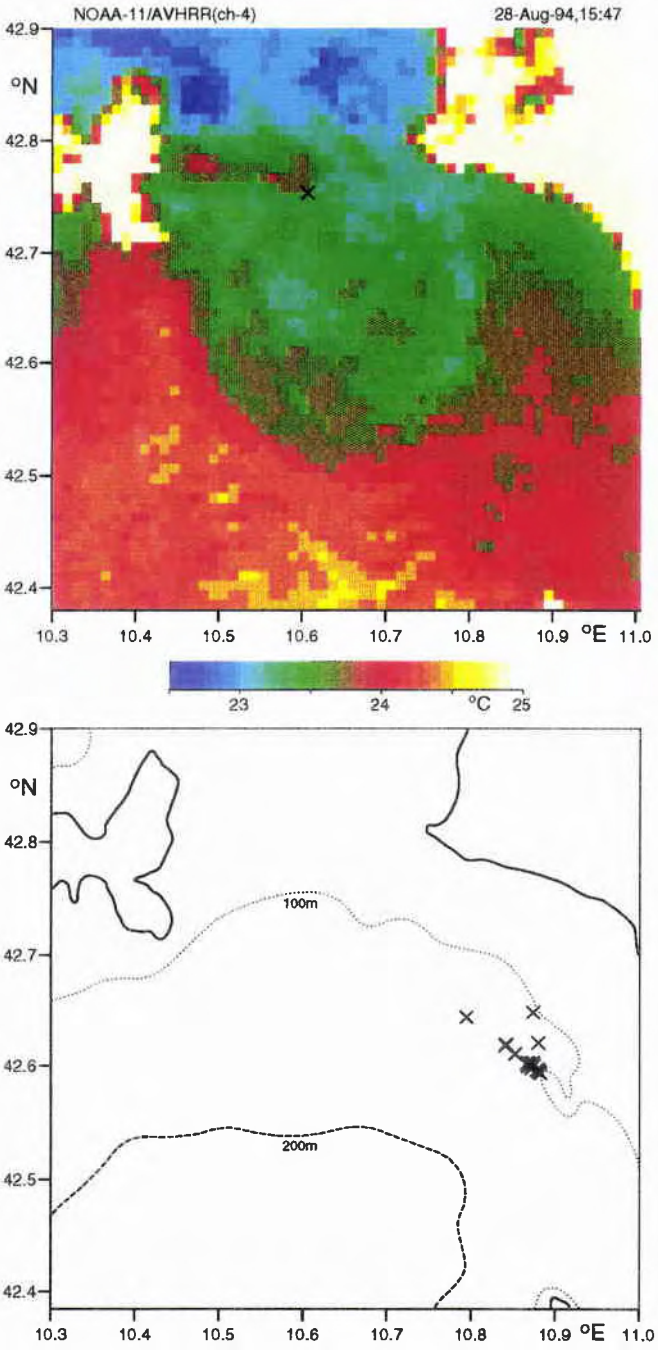

Figure 1: *Above: Channel-4 brightness temperatures from the Elba-94 experimental area. The position of NRV Alliance is marked by a cross. Below: Locations of the CTD casts (marked by crosses). Depth contours are drawn at* 100 m *(dotted lines) and* 200 m *(dashed lines).*

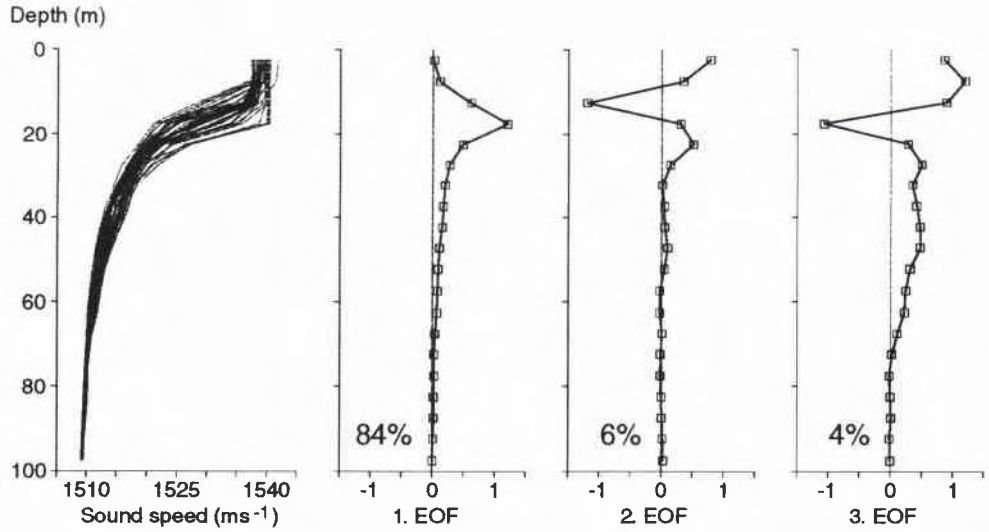

Figure 2: *EOF-decomposition of the Elba-94 sound-speed profiles. The left panel shows all the profiles used. The EOFs are displayed in the right panels together with the amount of variance they account for.*

Figure 3 compares the EOF-amplitudes with near-surface temperatures, measured at the uppermost layer of the CTD casts. As higher-order curves do not allow better fits, the results of linear regression are presented. There is no correlation between the 1st-order EOF amplitude and SST but a relatively high correlation between 2nd-order EOF amplitude and SST. But this correlation is not very useful, because the 2nd EOF accounts for only 6% of the sound-speed profile variance.

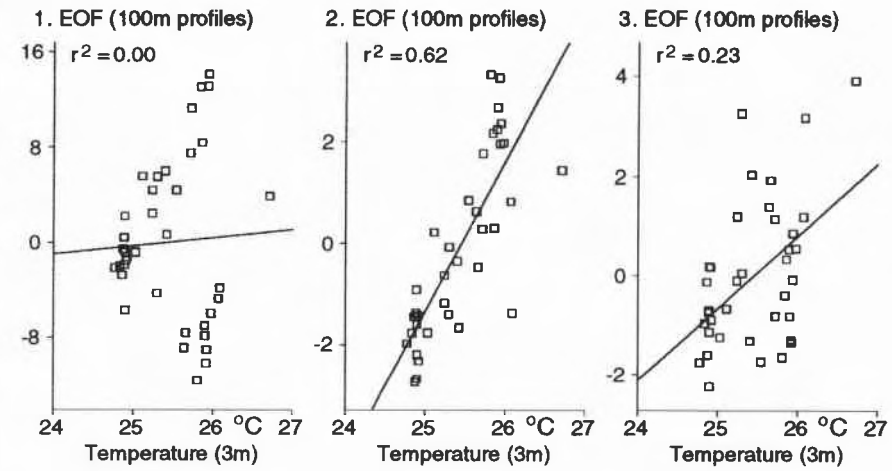

Figure 3: *First three EOF amplitudes of sound speed versus near-surface temperature from the Elba-94 experiment. Sound-speed profiles extend to* 100 m. *Linear regression curves have been used. See (5) for the definition of* r^2.

In order to demonstrate the contribution of each of the EOFs, synthetic profiles have been constructed in Fig. 4 by summing the mean profile and each EOF, the 1st, 2nd, or 3rd, with amplitudes varying in the same ranges as the amplitudes of the data. The 1st EOF nearly vanishes at the sea surface explaining the absence of correlation with SST. The 2nd EOF shows the strongest variations just below the sea surface. By correlation with SST these could be determined from satellite data, but this information is of limited value, because the 2nd EOF might be dominated by contributions of the other two EOFs.

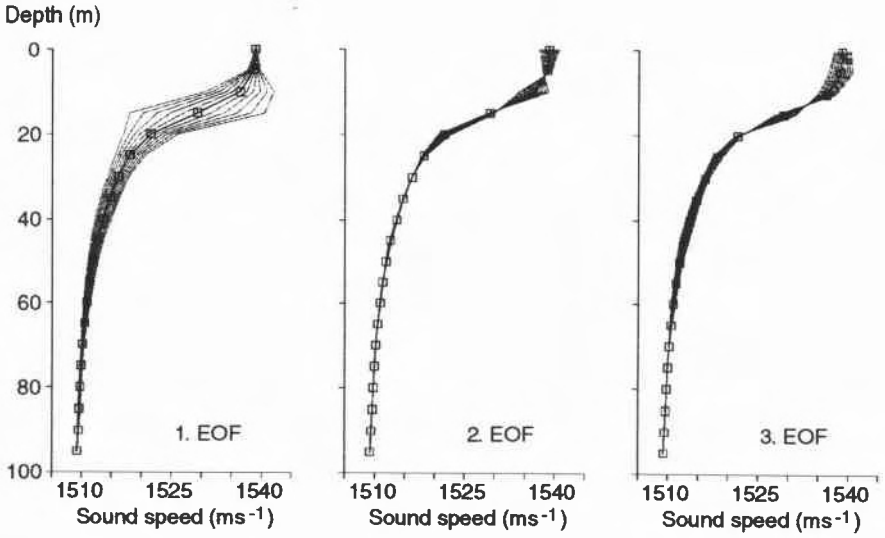

Figure 4: *Synthetic sound-speed profiles, demonstrating the amount of variability represented by the first three EOFs. The mean profile and each one EOF with varying amplitude are added.*

With the exception of one data point, the measured SST varies between 24.8°C and 26.1°C (Fig. 3), i.e. by 1.3°C only. This variability is mainly due to seasonal cooling (Fig. B1 in Annex B). The 1st EOF accounts for most of the sound-speed variability (Fig. 2), which obviously is due to the depth and shape of the thermocline (Fig. 4). These may not be observed from satellite-measured SST, because the 1st EOF amplitude is not correlated with SST (Fig. 3).

4.2 Sicily (Nov-94)

Fig. 5 (upper part) shows an AVHHR (channel-4) image of Sicily and the ocean to the south. The dark blue represents brightness temperatures below 12°C which indicate land or clouds. The position of NRV *Alliance* during the overpass of NOAA-12 is marked by a cross. The water temperature measured at 2 m below the sea surface was 20.2°C, and the channel-4 brightness temperature at this position 16.2°C, a difference of 4.0°C which is used for correcting the satellite temperatures.

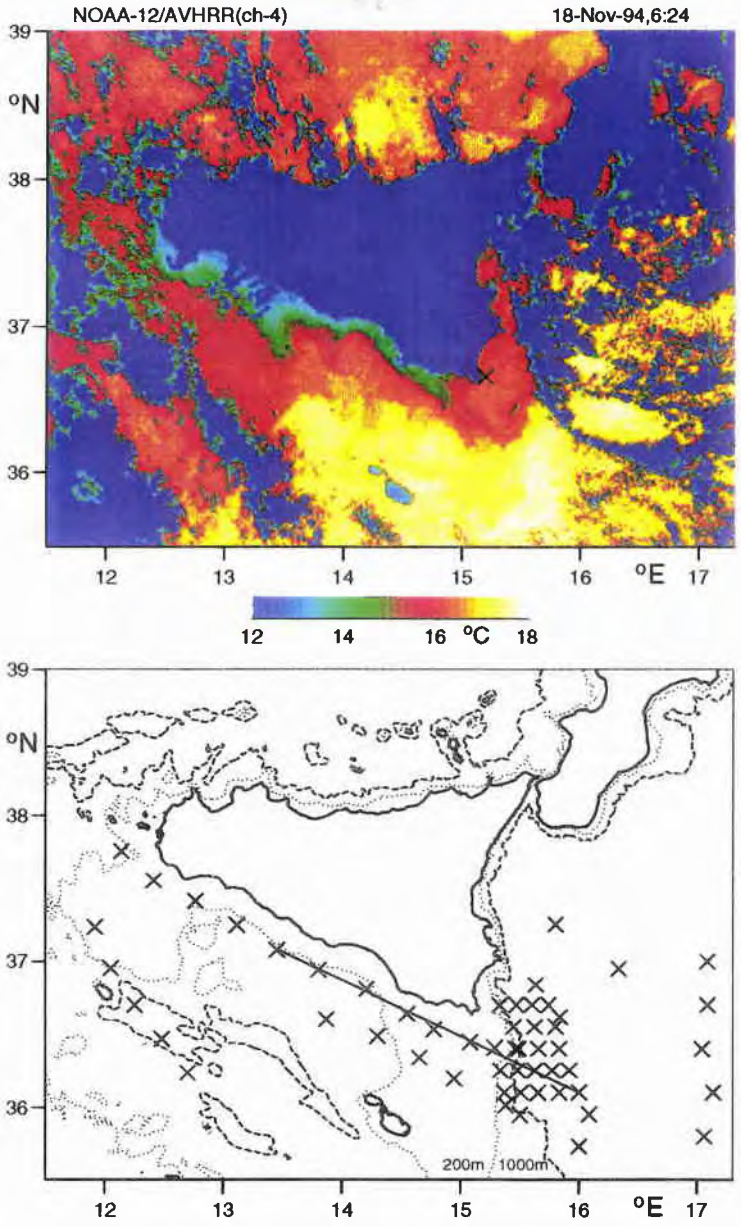

Figure 5: *Above: Channel-4 brightness temperatures from the Sicily-94 experimental area. The position of NRV Alliance is marked by a cross (near SW corner of Sicily). Below: Locations of the CTD casts (marked by crosses). Depth contours are drawn at* 200 m *(dotted lines) and* 1000 m *(dashed lines). The line indicates satellite-retrieved SSTs for subsequent analysis.*

Sixty CTD casts were carried out at depths from 40 m to 3670 m. The CTD measurements extend to about 15 m above the sea floor but not deeper than 750 m. Figure 5 (lower part) shows the bathymetry of the area and the positions of the CTD casts used for the EOF analysis, i.e. those which reach a depth of at least 75 m. Measuring times and coordinates are given in Table A2 of Annex A. The data cover an area of 400 km from west to east and some 200 km from south to north. The straight line in the lower part of Fig. 5 represents a cloud-free section, from which satellite SSTs have been collected for further analysis.

The EOF analysis requires that the profiles are of the same length and have to be cut off at a certain depth. In order to determine the influence of profile length, we consider two cases, extensions to 75 m and 300 m depth, respectively. Measurements, not reaching the profile length, are rejected. Of the 60 CTD stations, 55 remain for the 75 m profiles and 42 for the 300 m profiles. In order to limit the number of vertical horizons, sound speeds have been averaged into 5 m or 10 m intervals, respectively. Figure 6 presents the results of the EOF analysis for the 75 m and the 300 m profiles. The left panel displays all sound-speed profiles available. The first three EOFs are shown and account for 97% and 95% of the variance, respectively. It is remarkable that the 1st EOF of the 75 m profiles nearly coincides with that of the 300 m profiles and that the mean profiles deviate only slightly.

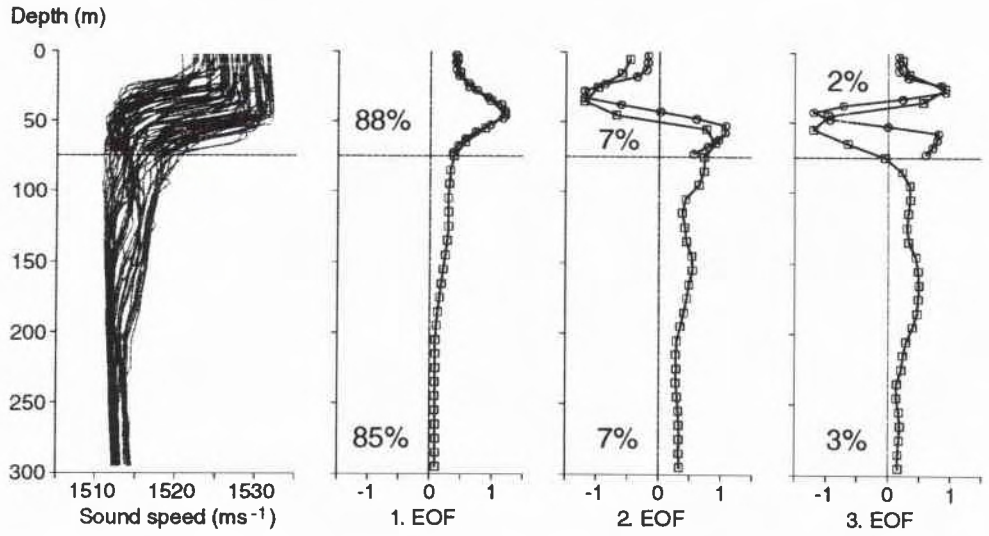

Figure 6: *EOF-decomposition of sound-speed profiles extending to at least* 75 m *and* 300 m *depth, repectively. The left panel shows the* 75 m *profiles with* 5 m *spacing and the* 300 m *profiles with* 10 m *spacing. The EOFs are displayed in the right panels together with the amount of variance they account for.* 75 m *profiles are indicated by circles,* 300 m *profiles by squares.*

Measured sound-speed profiles along the section (from west to east), indicated in the lower part of Fig. 5, are displayed in Fig. 7 together with reconstructed profiles representing the contribution of selected EOFs. Due to the relatively shallow water in this area a profile length of 75 m was selected. The sound-speed profiles change considerably with distance, as becomes clear by comparison with the mean profile (dotted line). Reconstruction by means of the 1st EOF (full line) already yields a good fit of overall features. The inclusion of the 2nd and 3rd EOF (dashed line) accounts for more variability.

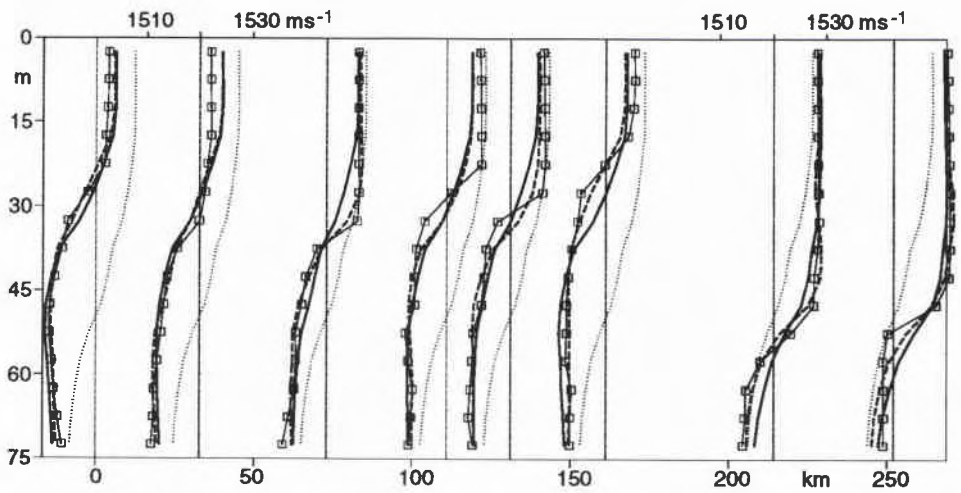

Figure 7: *Representation by EOFs of eight sound-speed profiles along the section indicated in Fig. 5. Lines marked by squares are the original data, thin dotted lines are the mean profile, full lines are the reconstruction by only the 1st EOF, dashed lines by the 1st through 3rd EOF.*

Figure 8 compares EOF amplitudes with near-surface temperatures. Because of a slight increase in r^2, quadratic regression curves have been used for 1st EOF. There is no important difference in correlation between the two profile lengths, 75 m and 300 m. Both show high correlation of 1st-order EOF amplitude with SST, but no significant correlation for the 2nd- and 3rd-order EOF amplitudes.

The upper panel of Fig. 9 displays the corrected SST as retrieved from the AVHRR along the section in Fig. 5. The crosses represent near-surface temperatures measured by the CTD sonde. Because these measurements have been taken several days before the satellite image, no exact agreement can be expected. However, there should be general agreement as our method assumes that the SST is representative for the subsurface sound speed. The lower panel shows synthetic sound-speed profiles computed every 6 km along the section. The profiles are composed of the mean profile and 1st EOF with amplitudes retrieved from the SST in the upper panel. Compared with the real data (Fig. 7) the synthetic profiles are considerably

smoothed, but nevertheless represent important features of the spatial variability.

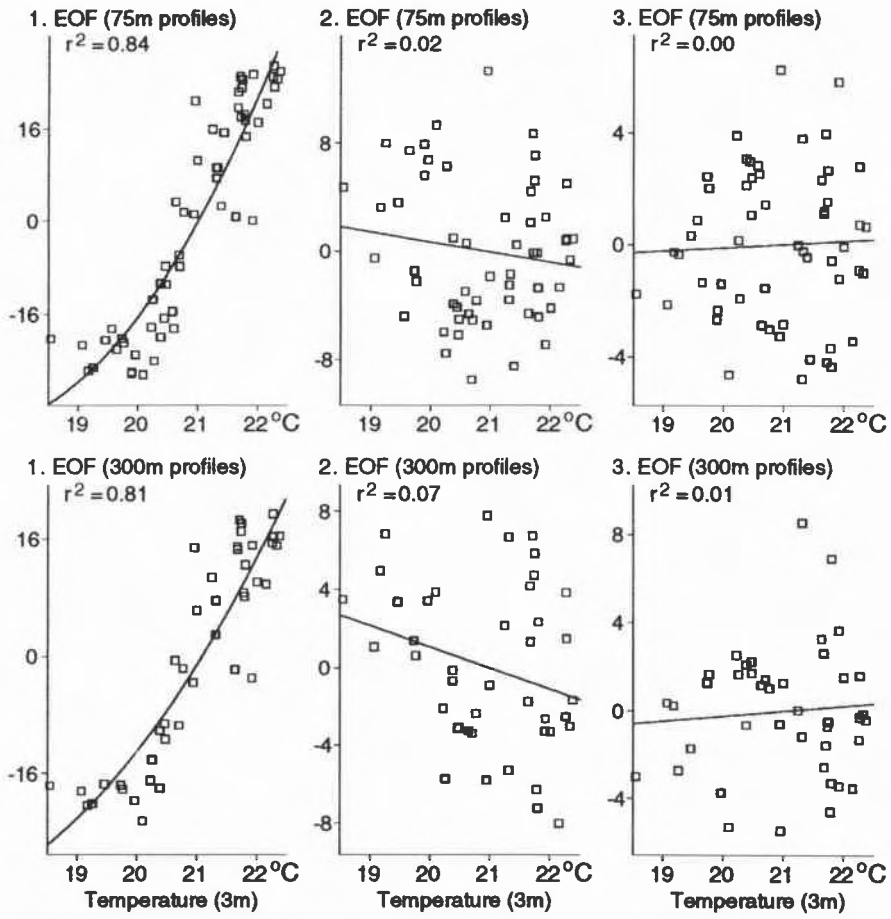

Figure 8: *First three EOF amplitudes of sound speed versus near-surface temperature from the Sicily-94 experiment. Upper and lower panels refer to sound-speed profiles extending to* 75 m *and* 300 m, *respectively. A quadratic regression curve has been used for 1st EOF and linear curves for 2nd EOF and 3rd EOF. See (5) for the definition of* r^2.

The area under investigation shows a high spatial variability of SST between 18.5°C and 22.5°C (Fig. B2 in Annex B). The amplitudes of 1st EOF, accounting for the major part of variance (Fig. 6), are highly correlated with SST (Fig. 8). These are optimal conditions for the determination of subsurface sound-speed features from satellite-retrieved SST.

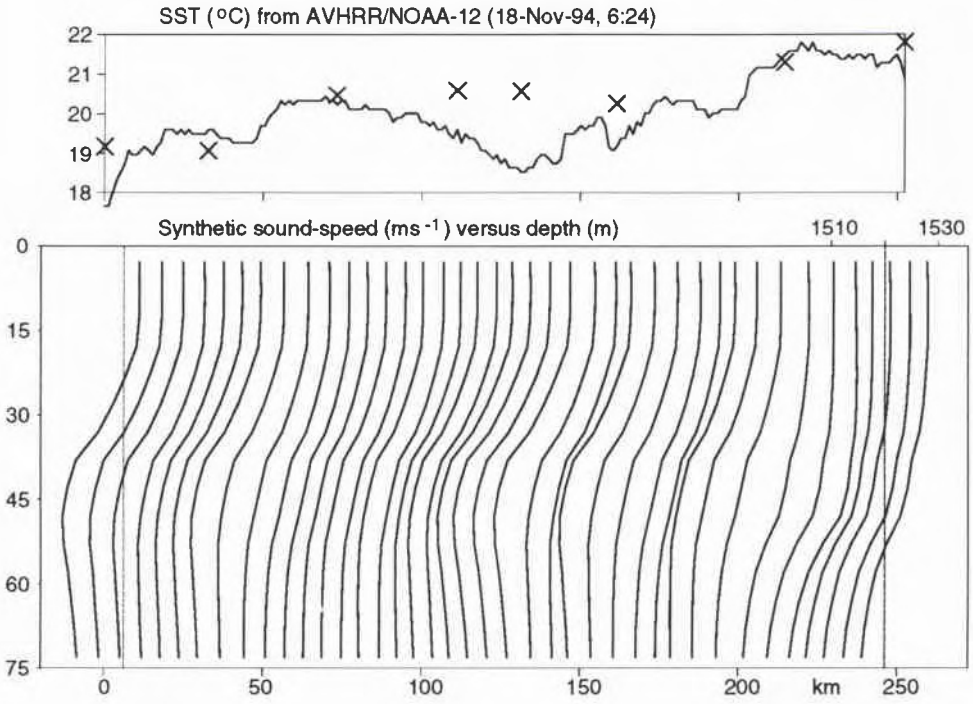

Figure 9: *Synthetic sound-speed profiles along the section shown in Fig. 5. Satellite SSTs are displayed in the upper panel, the crosses represent the CTD measurements. Sound-speed profiles every* 6 km *along the section have been derived from the mean profile and the 1st EOF, the amplitudes of which have been determined from satellite SSTs via the regression curve in Fig. 8.*

4.3 Elba (Apr/May-95)

The experimental area of the Elba-95 experiment is shown by the AVHRR image in the upper part of Fig. 10. Channel-4 brightness temperatures are displayed and the position of NRV *Alliance* is marked by a cross. The ship's measurement revealed 15.0°C, whereas the brightness temperature is 11.7°C at this postion, i.e. 3.3°C cooler. CTD casts were carried out for a period of 12 days, the positions of which are displayed in the lower part of Fig. 10 and listed in Table A3 of Annex A, together with measuring times. Only those casts which reach a depth of at least 100 m have been considered. The CTD measurements have been taken along the sides of a triangle with side lengths between 40 km and 55 km. Time intervals between the measurements are from less than 1 h up to 40 h.

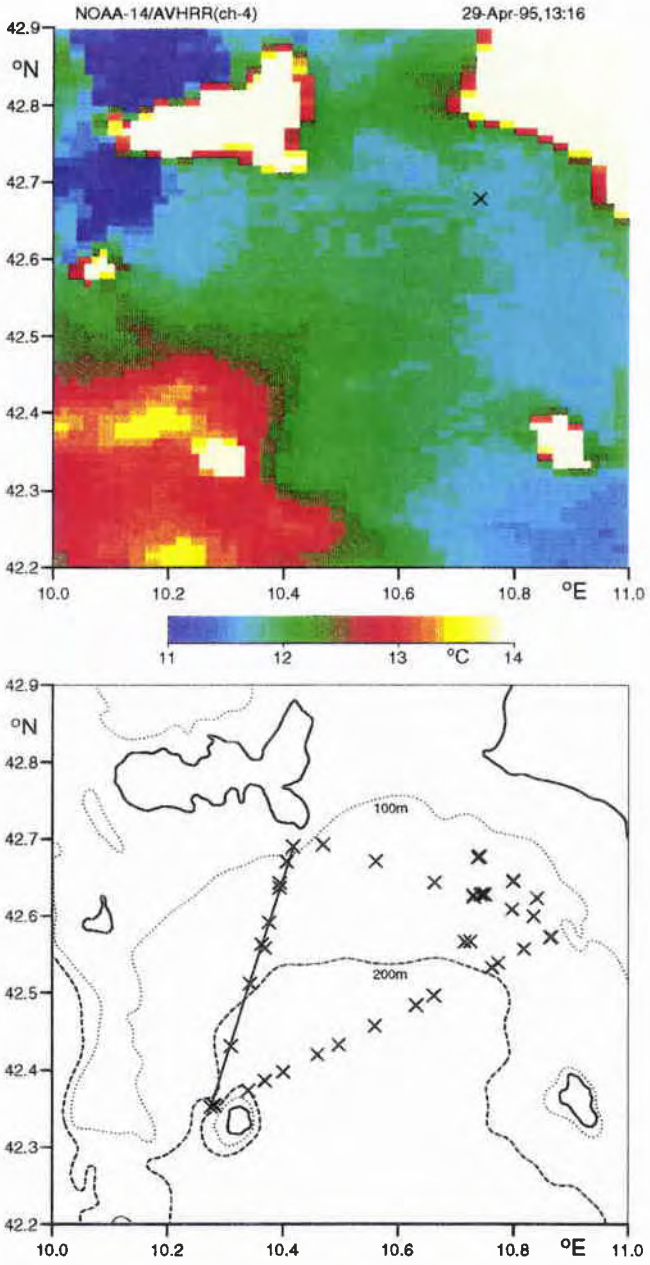

Figure 10: *Above: Channel-4 brightness temperatures from the Elba-95 experimental area. The position of NRV Alliance is marked by a cross. Below: Locations of the CTD casts (marked by crosses). Depth contours are drawn at* 100 m *(dotted lines) and* 200 m *(dashed lines). The line indicates satellite-retrieved SSTs for subsequent analysis.*

The EOF-decomposition in Fig. 11 reveals less variance for 1st EOF than the previous experiments. The shape of 1st EOF is different, with maximum amplitude at the sea surface and not in the thermocline. Figure 12 displays sound-speed profiles as measured along the section (from south to north), indicated in Fig. 10, together with reconstructed profiles. The sound-speed profiles show some variability along the section but deviate only by the order of 1 ms^{-1} from the mean profile. Reconstruction by means of 1st EOF is not satisfactory, the inclusion of the 2nd and 3rd EOF yields considerable improvements. This is due to the distribution of the sound-speed variance among the EOFs.

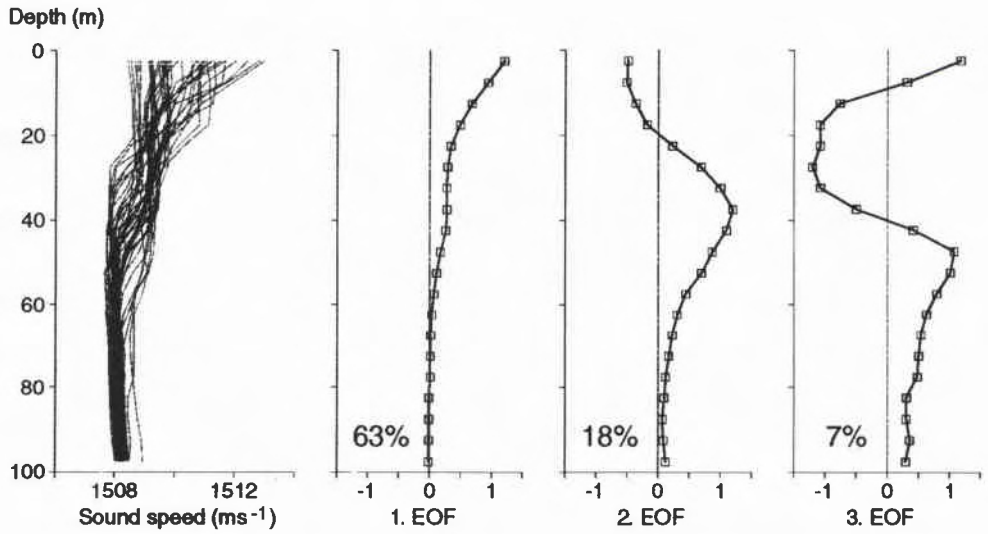

Figure 11: *EOF-decomposition of the Elba-95 sound-speed profiles. The left panel displays all profiles used. The EOFs are displayed in the right panels together with the amount of variance they account for.*

Figure 13 shows that the 1st-order EOF amplitude is highly correlated with SST, but that there is no significant correlation for the 2.- and 3rd-order EOF amplitudes. The upper panel of Fig. 14 displays the corrected SST as retrieved from the AVHRR along the section in Fig. 10. The crosses represent near-surface temperatures measured by the CTD sonde from 18 h before to 50 h after the satellite overpass. While the *in-situ* data reveal little variability, the satellite-retrieved SST decreases by about 2°C along the section. Regression analysis is based on temperatures in the range from 14°C to 16°C (Fig. 13). Synthetic profiles, spaced by 1.9 km along the section, determined from SSTs outside this interval are not reliable. For this reason they are represented by dashed lines (Fig. 14).

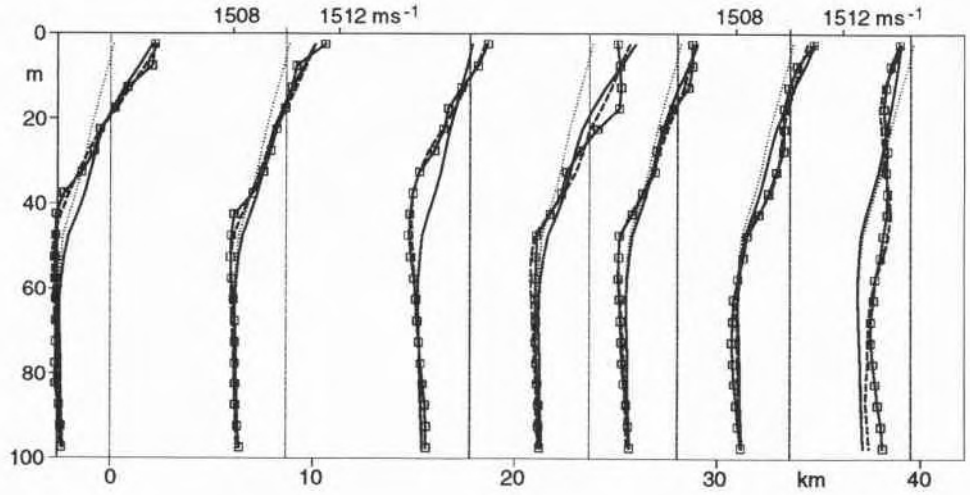

Figure 12: *Representation by EOFs of seven sound-speed profiles along the section indicated in Fig. 10. Lines marked by squares are the original data, thin dotted lines are the mean profile, full lines are the reconstruction from 1st EOF, dashed lines from 1st to 3rd EOF.*

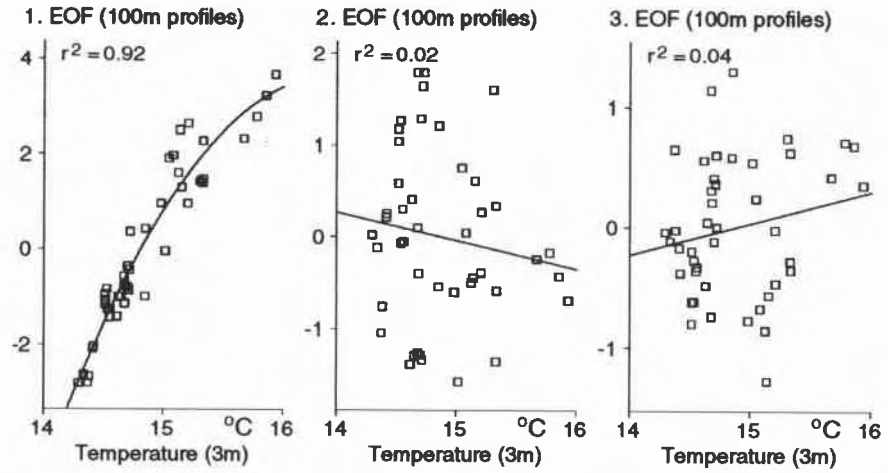

Figure 13: *First three EOF amplitudes of sound speed versus near-surface temperature from the Elba-95 experiment. Sound-speed profiles extend to* 100 m. *A quadratic regression curve has been used for 1st EOF and linear curves for 2nd EOF and 3rd EOF. See (5) for the definition of* r^2.

This data set is not appropriate for relating the variability of subsurface sound speed to SST, due to the lack of horizontal variablity. Except for the last 36 h of the experiment the ship-measured SST reveals no pronounced temperature fronts (Fig. B3 in Annex B). Though there is a high correlation between 1st-order EOF amplitude and SST (Fig. 13), the determination of synthetic sound speed profiles

is limited by the fact that 1st EOF accounts for only 63% of sound-speed variance (Fig. 11).

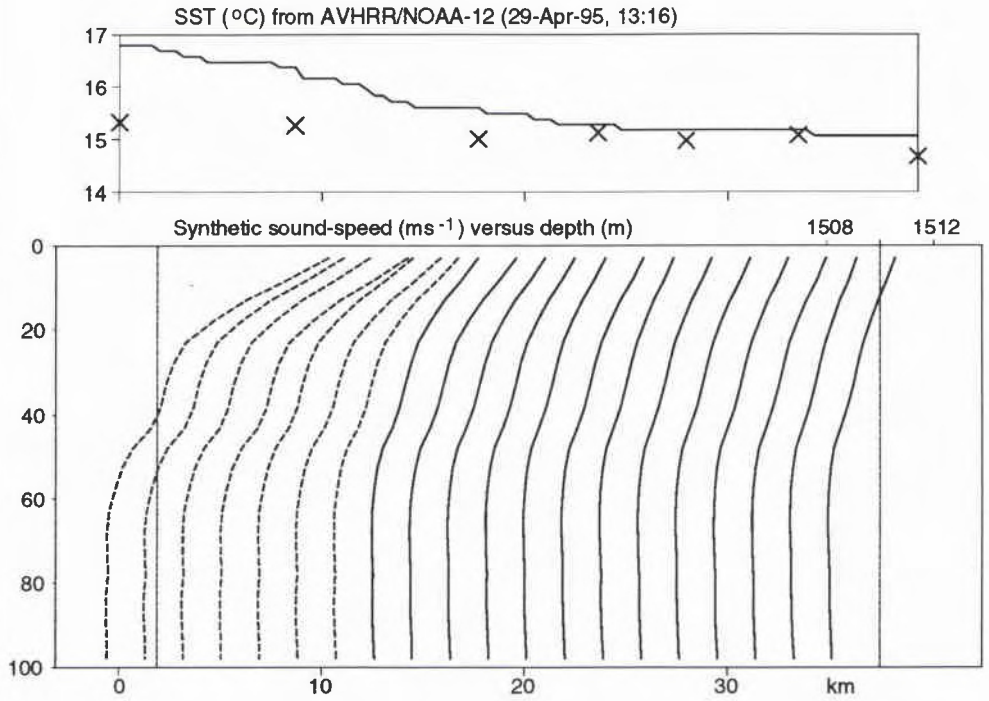

Figure 14: *Synthetic sound-speed profiles along the section shown in Fig. 10. Satellite SSTs are displayed in the upper panel, the crosses represent the CTD measurements. Sound-speed profiles every* 1.9 km *along the section have been derived from the mean profile and 1st EOF, the amplitudes of which have been determined from satellite SSTs via the regression curve in Fig. 13. Dashed profiles are constructed from SSTs exceeding the interval of CTD data.*

4.4 Otranto Gap (May-95)

The upper part of Fig. 15 shows an AVHRR (channel-4) image of the Otranto Gap. At the position of NRV *Alliance*, marked by a cross, the temperatures of adjacent pixels vary between 15.7°C and 15.9°C. The ship-measured SST reveals the same variablity around 18.6°C within a period of 20 min, 2.8°C warmer than the brightness temperature. Positions of the CTD casts, carried out by the two research vessels NRV *Alliance* and IRV *Magnaghi* used for the EOF analysis, are shown in the lower part of Fig. 15. Measuring times and coordinates are listed in Table A4 of Annex A.

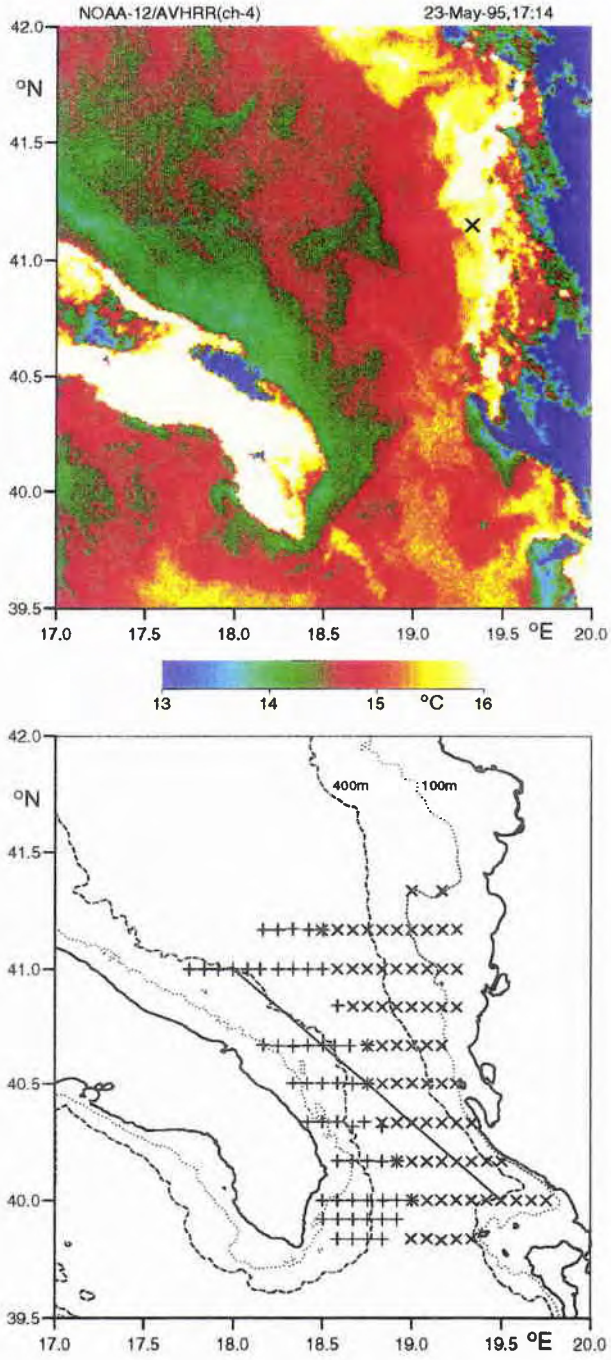

Figure 15: *Above: Channel-4 brightness temperatures from the Otranto-95 experimental area. The position of NRV Alliance is marked by a cross. Below: Locations of the CTD casts (marked by crosses). Depth contours are drawn at* 100 m *(dotted lines) and* 400 m *(dashed lines). The line indicates satellite-retrieved SSTs for subsequent analysis.*

The Otranto Gap area was completely surveyed within 106 h. The CTD measurements extend to just above the sea floor, which reaches a maximum depth of 1050 m. As for the Sicily area, two cases are considered, profiles extending to 75 m or to 300 m. The number of profiles available for each option are 130 and 76, respectively. Figure 16 presents the results of EOF analysis for the 75 m and the 300 m profiles. The left panel displays all sound-speed profiles available. Some of the 75 m profiles reveal lower sound-speeds at the depth of 75 m than the 300 m profiles, which leads to deviating EOFs. The first three EOFs account for 95% and 93% of the variance, respectively.

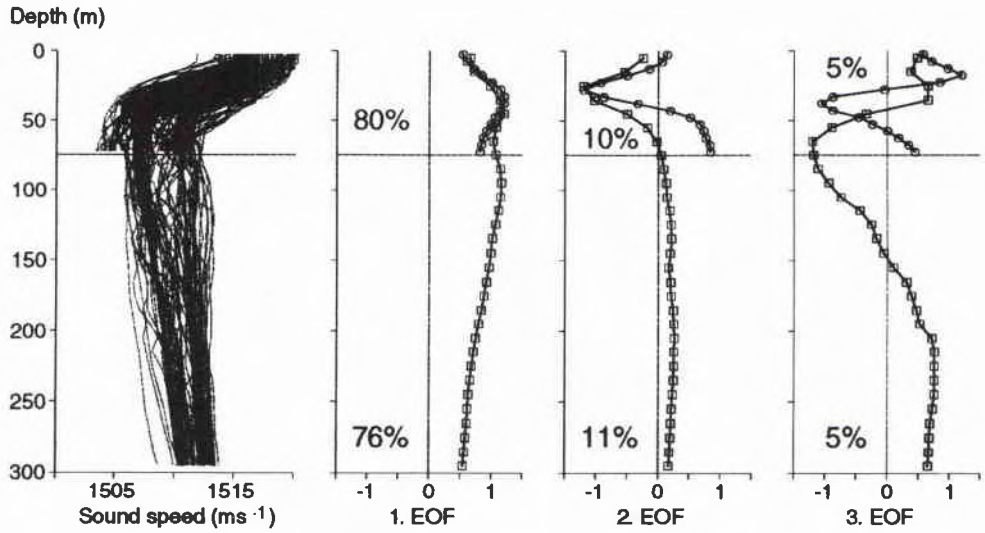

Figure 16: *EOF-decomposition of sound-speed profiles extending to 75m and 300m depth, repectively. The left panel shows the 75 m profiles with 5 m spacing and the 300 m profiles with 10 m spacing. The EOFs are displayed in the right panels together with the amount of variance they account for. 75 m profiles are indicated by circles, 300 m profiles by squares.*

Figure 17 displays measured and reconstructed sound-speed profiles along the section indicated in Fig. 15, from south-east to north-west through a deep trench. As the variability of sound speed extends to greater depths, the 300 m option has been been chosen. Reconstruction by means of 1st EOF yields highly smoothed curves. A somewhat better approximation is found by the inclusion of the 2nd and 3rd EOF, but some strong vertical gradients, especially the sound-speed ducts in the 1., 3. and 4. profile are smoothed out by the EOF-representation.

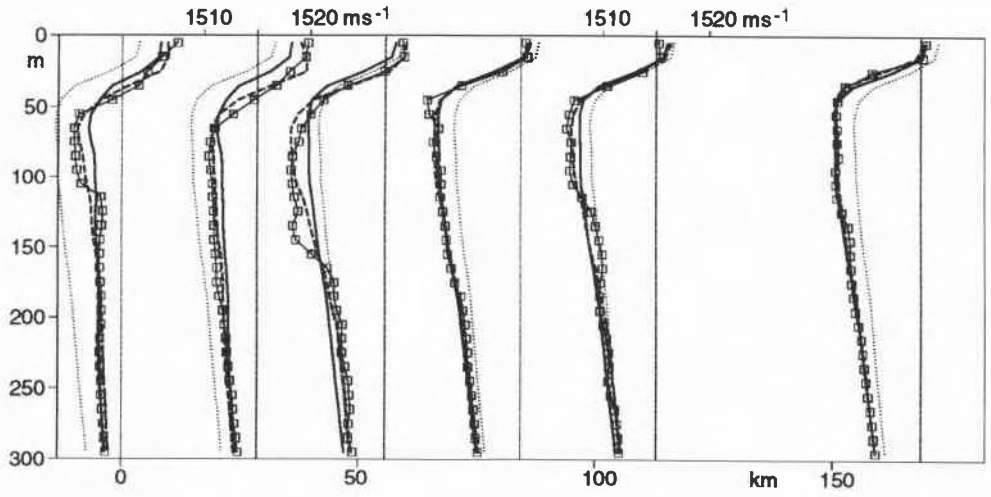

Figure 17: *Representation by EOFs of six sound-speed profiles along the section indicated in Fig. 15. Lines marked by squares are the original data, thin dotted lines are the mean profile, full lines are the reconstruction by 1st EOF, dashed lines by 1st to 3rd EOF.*

Significant correlation between EOF amplitudes and SST is found only for the 1st EOF (Fig. 18). Linear regression has been considered, as higher-order approaches do not allow better fits. The degree of correlation is similar for the two profile lengths, but less than that of the Sicily-94 experiment (Fig. 8). Figure 19 shows the attempt to determine sound-speed profiles along the section in Fig. 15 from satellite-retrieved SST. The upper panel displays the SST together with the data of the CTD sonde (crosses), of which the last one has been taken about 1*h* after the satellite overpass, and is 0.6°C cooler than the corrected satellite SST. This discrepancy may be caused by horizontal advection or inaccuracy in the image navigation, but more likely by different atmospheric influences on the satellite data at the positions of NRV *Alliance* and IRV *Magnaghi*.

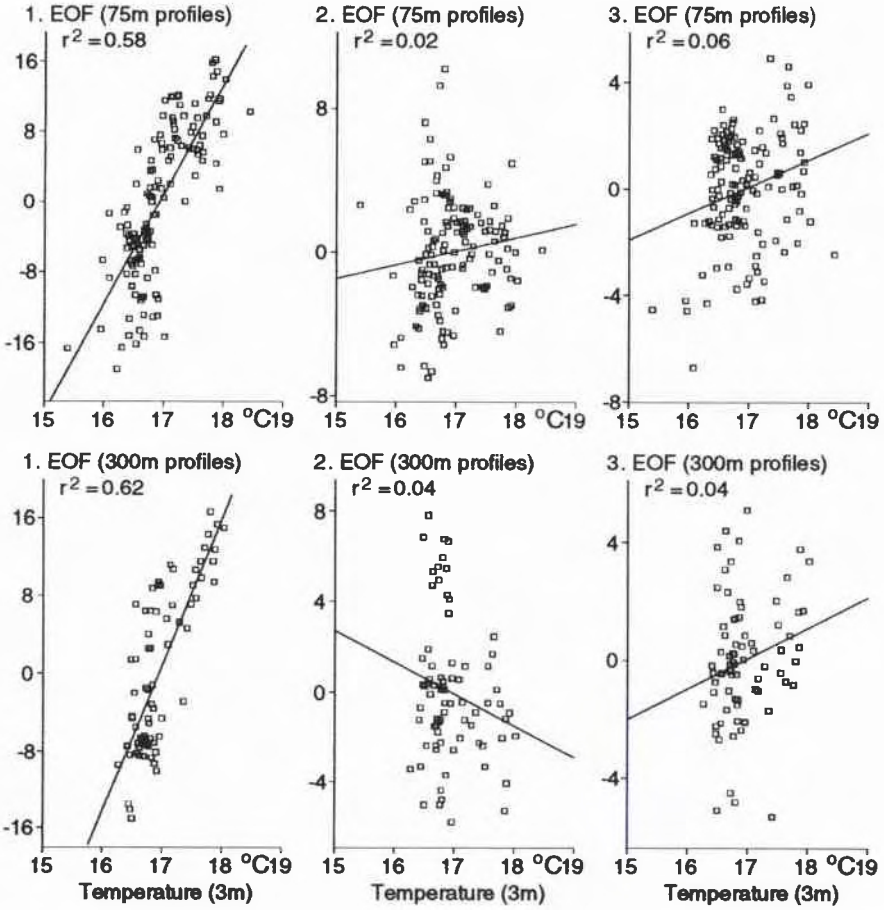

Figure 18: *First three EOF amplitudes of sound speed versus near-surface temperature from the Otranto-95 experiment. Upper and lower panels refer to sound-speed profiles extending to* 75 m *and* 300 m, *respectively. Linear regression curves have been used. See (5) for the definition of* r^2.

The low variability of SST of 1.2°C along the section and errors of the satellite data of some ±0.5°C considerably reduce the possibility of determining subsurface features of sound-speed. As important features of the sound-speed profiles are smoothed out by the 1st EOF (Fig. 17), and it is only weakly correlated with SST (Fig. 18), the synthetic profiles every 5.4 km along the section in Fig. 19 do not represent well the measured data in Fig. 17.

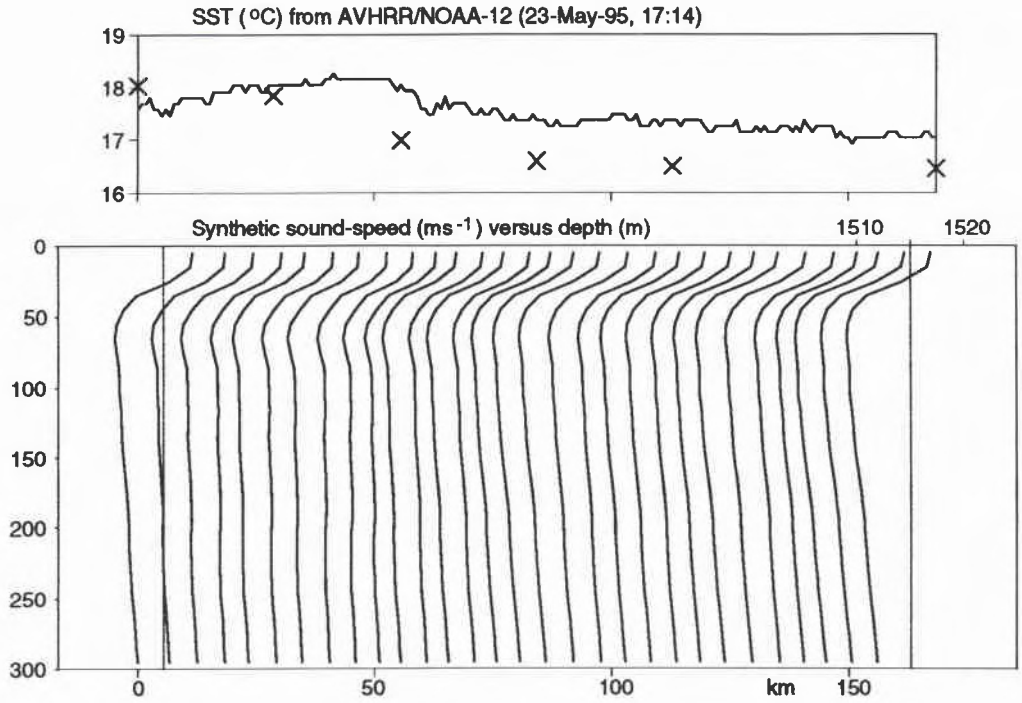

Figure 19: *Synthetic sound-speed profiles along the section shown in Fig. 15. Satellite-retrieved SSTs are displayed in the upper panel, the crosses represent the CTD-measured SSTs. Sound-speed profiles every* 5.4 km *along the section have been constructed by means of the mean profile and the 1st EOF, the amplitudes of which have been determined from satellite SSTs via the regression curve in Fig. 18.*

5 Conclusions

This report investigates the possibility of determining features of subsurface sound speed from satellite-measured sea-surface temperature. The method used is based on the decomposition of sound-speed profiles into EOFs and the correlation of their amplitudes with SST. Data from four hydrographic surveys in the Mediterranean have been analysed. In all cases, the first three EOFs account for at least 88% of the variance of the sound-speed variability, but with different contributions from single EOFs. Significant correlation between EOF amplitudes and SST has been found for only one of the three first EOFs, either 1st EOF or 2nd EOF. The second case refers to the Elba-94 experiment, which surveyed temporal but not spatial variability.

No sound-speed features from SST could be determined for the Elba-94 experiment because the 1st EOF accounts for most of the variance but is not correlated with SST. Most of the area investigated during the Elba-95 experiment shows only little variability of SST ($\pm 1°C$), which in addition is biased by the seasonal warming of the sea surface. The 1st-order EOF amplitude is highly correlated with SST but the 1st EOF accounts for only 63% of sound-speed variance. Taking into account the accuracy of the satellite retrieved SST ($\pm 0.5°C$), it is unlikely that SST yields reliable information on subsurface sound-speed.

The Sicily-94 experiment reveals SST variability of $\pm 2°C$, mainly due to spatial changes. The 1st EOF accounts for almost 88% of the variance and its amplitude is highly correlated with SST. These conditions allow the determination of subsurface sound-speed features, mainly long-scale variability. The spatial variability of SST during the Otranto-95 experiment is $\pm 1.5°C$. But in contrast to the Sicily-94 experiment, single sound-speed profiles show rapid vertical changes, due to a more complicated structure of the water mass. The 1st EOF accounts for 80% of variance and its amplitude is only weakly correlated with SST. For this reason the determination of synthetic sound-speed profiles from SST for this case yields no satisfactory result.

Only one of four data sets allows retrieval of subsurface sound speed from SST. The method requires knowledge of spatial changes in SST which exceed the accuracy of satellite-retrieved values. In addition, the composition of the water mass should allow the vertical sound-speed profiles to be relatively smooth. These conditions were fulfilled only during the Sicily-94 experiment.

References

[1] Carnes, M.R., Mitchell, J.L, deWitt, P.B. (1990). Synthetic temperature profiles derived from Geosat altimetry: Comparison with air-dropped expendable bathythermograph profiles. *Journal of Geophysical Research*, **95**, 17979-17992.

[2] Essen, H.H., Sellschopp, J. (1994). Three-dimensional distribution of sound speed in the Iceland-Faeroe area, retrieved from a CTD survey, thermistor-chain measurements and satellite SST imagery, SACLANTCEN SR-226. La Spezia, Italy, SACLANT Undersea Research Centre.

[3] Brekhovskikh, L.M., Lysanov, Y.P. (1991). Fundamentals of Ocean Acoustics, 2nd edition. Berlin, Springer Verlag.

[4] Minnett, P.J. (1991). Surface measurements made during the Icelandic Current Experiment (ICE 89) from the R/V *Alliance*, SACLANTCEN SM-247. La Spezia, Italy, SACLANT Undersea Research Centre.

A

Lists of CTD casts

This annex contains times and positions of the CTD casts and time-series of surface meteorological measurements. Only profiles which have been used for the EOF analysis are listed in Tables A1,..,A4. The criteria for selection are the extension to a certain depth (100 m for the two Elba experiments, 75 m for the Sicily and Otranto experiments) and if taken at the same position, a temporal separation of at least 1 h.

day	hour	lat.	long.	day	time	lat.	long.
28 Aug	12:11	42.594	10.882	03 Sep	11:08	42.602	10.871
28 Aug	13:18	42.644	10.794	03 Sep	12:09	42.601	10.871
30 Aug	12:30	42.611	10.852	03 Sep	13:09	42.600	10.874
30 Aug	13:29	42.611	10.852	03 Sep	14:09	42.603	10.866
30 Aug	14:29	42.611	10.852	03 Sep	15:19	42.602	10.868
30 Aug	15:39	42.611	10.852	03 Sep	16:18	42.601	10.870
30 Aug	17:16	42.611	10.852	03 Sep	17:21	42.601	10.870
30 Aug	18:24	42.598	10.872	06 Sep	11:28	42.595	10.881
31 Aug	10:49	42.597	10.878	07 Sep	08:49	42.618	10.841
31 Aug	11:59	42.596	10.879	07 Sep	09:47	42.619	10.841
31 Aug	13:09	42.597	10.879	07 Sep	10:49	42.619	10.841
31 Aug	14:19	42.596	10.879	07 Sep	11:57	42.619	10.841
01 Sep	13:39	42.621	10.880	07 Sep	13:19	42.619	10.841
01 Sep	14:58	42.648	10.874	07 Sep	14:19	42.619	10.841
02 Sep	07:34	42.600	10.873	07 Sep	15:19	42.619	10.841
02 Sep	11:20	42.603	10.873	07 Sep	16:39	42.619	10.841
02 Sep	14:59	42.602	10.867	07 Sep	17:59	42.619	10.841
02 Sep	16:14	42.600	10.867	07 Sep	18:57	42.619	10.841
02 Sep	17:14	42.601	10.870	07 Sep	19:59	42.619	10.841

Table A1: *Elba-94 experiment CTD profiles*

day	hour	lat.	long.	day	time	lat.	long.
13 Nov	01:06	37.757	12.139	16 Nov	12:17	36.100	15.832
13 Nov	05:16	37.232	11.918	16 Nov	13:30	36.101	16.000
13 Nov	07:46	37.548	12.413	16 Nov	14:46	36.250	15.916
13 Nov	10:05	37.409	12.765	16 Nov	15:53	36.250	15.771
13 Nov	13:30	36.952	12.050	16 Nov	17:02	36.251	15.625
13 Nov	15:18	36.700	12.252	16 Nov	18:09	36.251	15.479
13 Nov	19:56	37.245	13.116	16 Nov	19:18	36.250	15.333
13 Nov	22:39	37.076	13.449	16 Nov	20:59	36.399	15.463
14 Nov	03:21	36.466	12.481	16 Nov	22:12	36.400	15.655
14 Nov	05:24	36.234	12.700	16 Nov	23:21	36.399	15.831
14 Nov	10:43	36.941	13.801	17 Nov	00:41	36.550	15.802
14 Nov	13:47	36.807	14.207	17 Nov	01:59	36.549	15.622
14 Nov	15:44	36.600	13.866	17 Nov	03:15	36.549	15.444
14 Nov	17:44	36.484	14.301	17 Nov	06:15	36.699	15.327
14 Nov	19:21	36.639	14.550	17 Nov	07:24	36.701	15.469
14 Nov	21:08	36.532	14.773	17 Nov	08:19	36.701	15.601
14 Nov	22:15	36.337	14.652	17 Nov	09:25	36.700	15.741
14 Nov	23:40	36.194	14.945	17 Nov	14:56	36.998	17.085
15 Nov	01:28	36.444	15.079	17 Nov	23:02	36.701	17.084
15 Nov	22:02	36.407	15.285	18 Nov	13:42	36.398	17.042
15 Nov	23:56	36.015	15.380	18 Nov	21:59	36.100	17.135
16 Nov	02:58	35.733	16.001	19 Nov	11:54	35.800	17.058
16 Nov	04:55	35.953	16.085	21 Nov	11:22	36.399	15.487
16 Nov	07:41	35.950	15.501	21 Nov	16:15	36.617	15.835
16 Nov	09:12	36.099	15.367	21 Nov	20:01	36.949	16.333
16 Nov	09:58	36.101	15.505	21 Nov	23:48	37.250	15.802
16 Nov	11:01	36.100	15.653	22 Nov	03:26	36.838	15.634

Table A2: *Sicily-94 experiment CTD profiles*

day	hour	lat.	long.	day	time	lat.	long.
21 Apr	11:57	42.356	10.282	27 Apr	13:25	42.644	10.663
21 Apr	14:17	42.354	10.282	28 Apr	20:02	42.690	10.418
22 Apr	12:03	42.623	10.840	29 Apr	10:05	42.677	10.738
23 Apr	14:00	42.600	10.835	29 Apr	12:58	42.678	10.741
24 Apr	09:53	42.387	10.369	29 Apr	15:28	42.678	10.740
24 Apr	10:58	42.433	10.497	29 Apr	17:23	42.646	10.799
24 Apr	12:00	42.484	10.632	29 Apr	19:57	42.645	10.799
24 Apr	12:57	42.539	10.773	30 Apr	06:21	42.352	10.275
24 Apr	13:43	42.573	10.864	30 Apr	07:29	42.431	10.310
24 Apr	15:29	42.573	10.866	30 Apr	08:13	42.512	10.344
26 Apr	07:23	42.373	10.341	30 Apr	09:01	42.592	10.376
26 Apr	07:56	42.386	10.370	30 Apr	09:46	42.671	10.407
26 Apr	08:31	42.398	10.401	01 May	10:50	42.558	10.369
26 Apr	09:33	42.420	10.460	01 May	12:29	42.563	10.364
26 Apr	10:43	42.457	10.560	01 May	15:10	42.637	10.394
26 Apr	11:46	42.496	10.662	01 May	16:29	42.643	10.395
26 Apr	12:43	42.533	10.762	02 May	06:05	42.693	10.470
26 Apr	13:18	42.557	10.818	02 May	09:18	42.672	10.561
26 Apr	21:40	42.567	10.725	02 May	12:29	42.628	10.750
26 Apr	22:17	42.566	10.715	02 May	14:20	42.628	10.742
27 Apr	12:14	42.608	10.797	02 May	16:30	42.629	10.746
27 Apr	12:48	42.625	10.731	02 May	17:50	42.627	10.730

Table A3: *Elba-95 experiment CTD profiles*

day	hour	lat.	long.	day	time	lat.	long.
19 May	22:16	39.835	19.332	22 May	06:56	40.500	18.750
19 May	23:28	39.833	19.249	22 May	11:12	40.667	19.167
20 May	00:50	39.829	19.163	22 May	11:56	40.667	19.083
20 May	02:33	39.834	19.083	22 May	12:45	40.667	19.001
20 May	04:11	39.835	18.997	22 May	13:43	40.667	18.916
20 May	10:50	40.000	19.750	22 May	15:08	40.667	18.834
20 May	11:38	40.000	19.667	22 May	16:11	40.665	18.750
20 May	12:44	39.999	19.583	22 May	19:32	40.832	19.250
20 May	13:44	39.999	19.499	22 May	20:18	40.833	19.167
20 May	14:42	40.000	19.416	22 May	20:58	40.833	19.083
20 May	15:41	40.001	19.332	22 May	21:37	40.834	18.999
20 May	17:13	40.001	19.248	22 May	22:21	40.834	18.917
20 May	18:23	40.001	19.163	22 May	23:09	40.834	18.833
20 May	19:45	40.000	19.084	23 May	00:14	40.835	18.750
20 May	20:52	40.000	19.003	23 May	01:41	40.836	18.669
21 May	01:18	40.168	19.500	23 May	06:02	41.000	19.251
21 May	02:33	40.167	19.417	23 May	06:37	41.000	19.168
21 May	03:43	40.167	19.333	23 May	07:32	41.000	19.085
21 May	05:07	40.166	19.249	23 May	08:14	41.001	19.001
21 May	06:17	40.166	19.166	23 May	09:12	41.000	18.913
21 May	07:39	40.166	19.083	23 May	10:00	41.000	18.833
21 May	08:44	40.166	19.000	23 May	10:58	41.000	18.749
21 May	10:00	40.167	18.917	23 May	11:50	41.000	18.666
21 May	13:24	40.332	19.334	23 May	12:53	41.000	18.581
21 May	14:18	40.333	19.250	23 May	18:12	41.168	19.250
21 May	15:11	40.333	19.166	23 May	19:00	41.168	19.168
21 May	16:40	40.333	19.083	23 May	19:36	41.167	19.083
21 May	18:20	40.334	19.003	23 May	20:11	41.167	18.999
21 May	19:34	40.333	18.918	23 May	20:55	41.167	18.916
21 May	20:40	40.333	18.833	23 May	21:33	41.167	18.833
22 May	00:32	40.501	19.244	23 May	22:27	41.167	18.750
22 May	01:22	40.500	19.167	23 May	23:18	41.167	18.667
22 May	02:14	40.500	19.084	24 May	00:36	41.167	18.582
22 May	03:15	40.502	19.002	24 May	01:52	41.165	18.494
22 May	04:39	40.501	18.917	24 May	07:26	41.333	19.166
22 May	05:41	40.500	18.834	24 May	08:22	41.333	18.999

Table A4a: *Otranto-95 experiment CTD profiles (NRV Alliance)*

day	hour	lat.	long.	day	time	lat.	long.
20 May	07:32	39.833	18.834	22 May	09:19	40.500	18.667
20 May	08:46	39.833	18.750	22 May	10:38	40.502	18.584
20 May	09:53	39.833	18.667	22 May	11:23	40.501	18.499
20 May	10:55	39.833	18.583	22 May	12:07	40.502	18.413
20 May	12:47	39.918	18.501	22 May	13:01	40.502	18.333
20 May	13:28	39.918	18.585	22 May	17:37	40.669	18.750
20 May	14:07	39.918	18.668	22 May	20:52	40.667	18.650
20 May	14:52	39.918	18.752	22 May	22:01	40.667	18.567
20 May	15:46	39.918	18.835	22 May	22:48	40.668	18.501
20 May	17:06	39.918	18.918	22 May	23:27	40.668	18.418
20 May	21:06	40.000	19.000	22 May	00:08	40.665	18.334
20 May	22:50	40.001	18.918	23 May	00:47	40.666	18.251
21 May	00:31	39.999	18.838	23 May	01:27	40.669	18.169
21 May	02:27	40.000	18.750	23 May	04:41	40.840	18.584
21 May	03:42	40.000	18.667	23 May	13:19	41.000	17.756
21 May	04:38	40.000	18.583	23 May	14:08	41.000	17.839
21 May	05:40	40.000	18.500	23 May	14:51	41.000	17.917
21 May	10:19	40.169	18.919	23 May	16:23	41.000	18.000
21 May	12:15	40.168	18.833	23 May	17:06	41.000	18.083
21 May	13:34	40.168	18.751	23 May	18:09	41.000	18.150
21 May	14:42	40.168	18.667	23 May	19:09	41.000	18.250
21 May	15:30	40.168	18.584	23 May	20:36	41.000	18.333
21 May	21:32	40.317	18.833	23 May	21:45	41.000	18.417
21 May	22:51	40.337	18.733	23 May	23:04	41.000	18.500
22 May	00:09	40.317	18.667	24 May	02:11	41.168	18.500
22 May	01:12	40.338	18.583	24 May	03:23	41.168	18.422
22 May	01:50	40.338	18.500	24 May	04:54	41.171	18.331
22 May	02:49	40.338	18.417	24 May	06:52	41.168	18.248
22 May	07:56	40.500	18.750	24 May	08:15	41.168	18.167

Table A4b: *Otranto-95 experiment CTD profiles (ITS Magnaghi)*

B

Surface meteorological data

This annex displays time series of air- and water temperature, relative humidity and wind speed, as recorded on NRV *Alliance* during hydrographic measurements. The data presented are averages over 1 min, taken at intervals of 5 min. The wind vector measured onboard the ship has been corrected by the ship's velocity. During rapid manoeuvres this procedure may cause errors, i.e. spikes in the time series. Due to malfunctioning of the navigation system, wind data are lacking for short time periods.

Figure B1 shows the meteorological data of the Elba-94 experiment. Relatively strong winds occurred between 1 and 3 September 1994, the air temperature dropped considerably, and afterwards the daily cycle became more pronounced. The water temperature shows short-period fluctuations of some 1°C, due to the ship crossing temperature fronts. Over the period there is a nearly continuous decrease of water temperature due to seasonal cooling.

The water temperature of the Sicily-94 experiment (Fig. B2) shows no seasonal trend. Rapid changes are due to the spatial variability, and probably the slight increase of mean temperature during the first three days of the time series, when the ship moved from about 12°E to 15°E. Wind speeds ranged from 5 ms^{-1} to 10 ms^{-1}, except for 14 November 1994 with lower winds and a 24 h period of high winds, starting 19 November at noon and reaching speeds of 18 ms^{-1}.

The mean wind speed during the Elba-95 experiment (Fig. B3) is about 5 ms^{-1}, maximum wind speeds reach 15 ms^{-1} for a period of 24 h starting 24 April 1995 at noon. The water temperature reveals only little variability, nearly no fronts, but a slight increase over the experiment, due to seasonal warming.

The 5-day period of the Otranto-95 experiment (Fig. B4) is characterized by three wind-speed regimes, starting with 42 h of winds between 6 ms^{-1} and 9 ms^{-1}, followed by 60 h of relative strong winds reaching speeds of 12 ms^{-1}, and finally 18 h of calm weather with wind speeds around 3 ms^{-1}. The water temperature reveals rapid changes of the order of 2°C, i.e. the presence of horizontal variability.

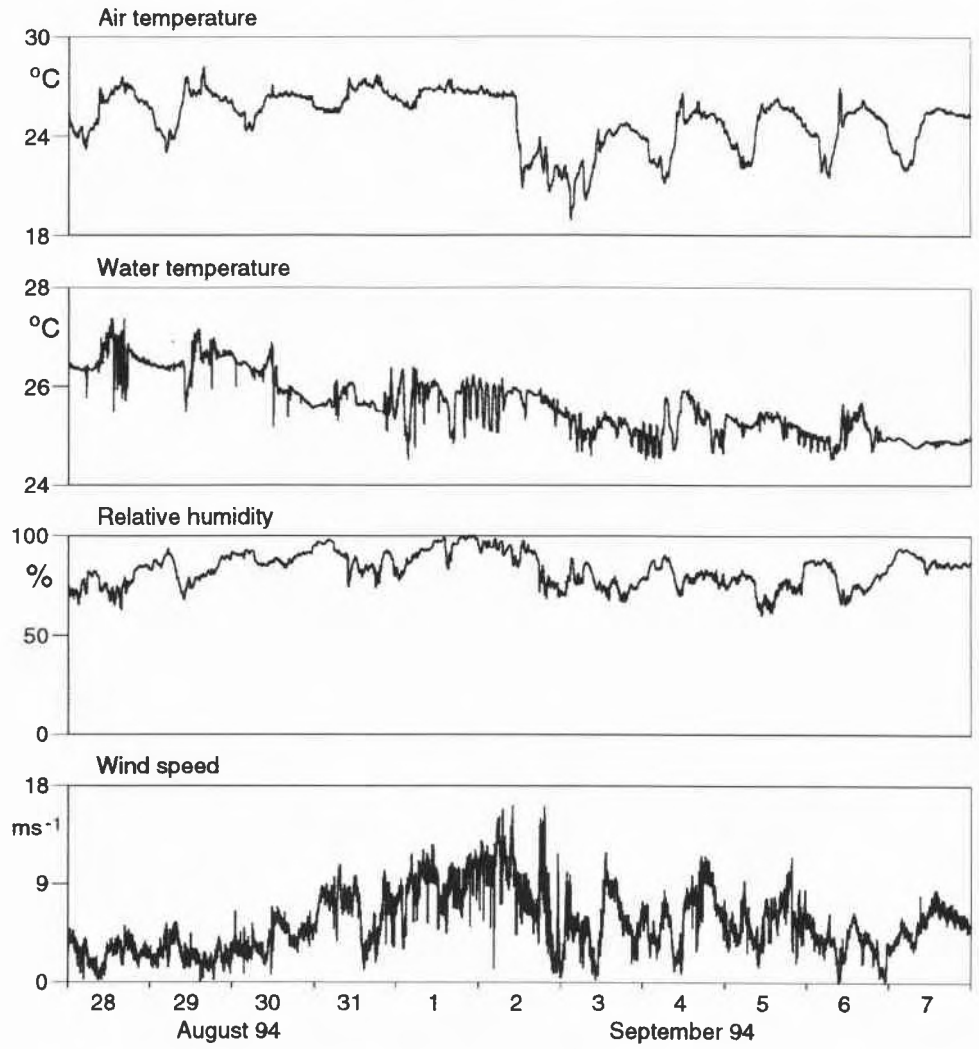

Figure B1: *Ship-borne measurements of air- and water-temperature, relative humidity and wind speed during the Elba-94 experiment.*

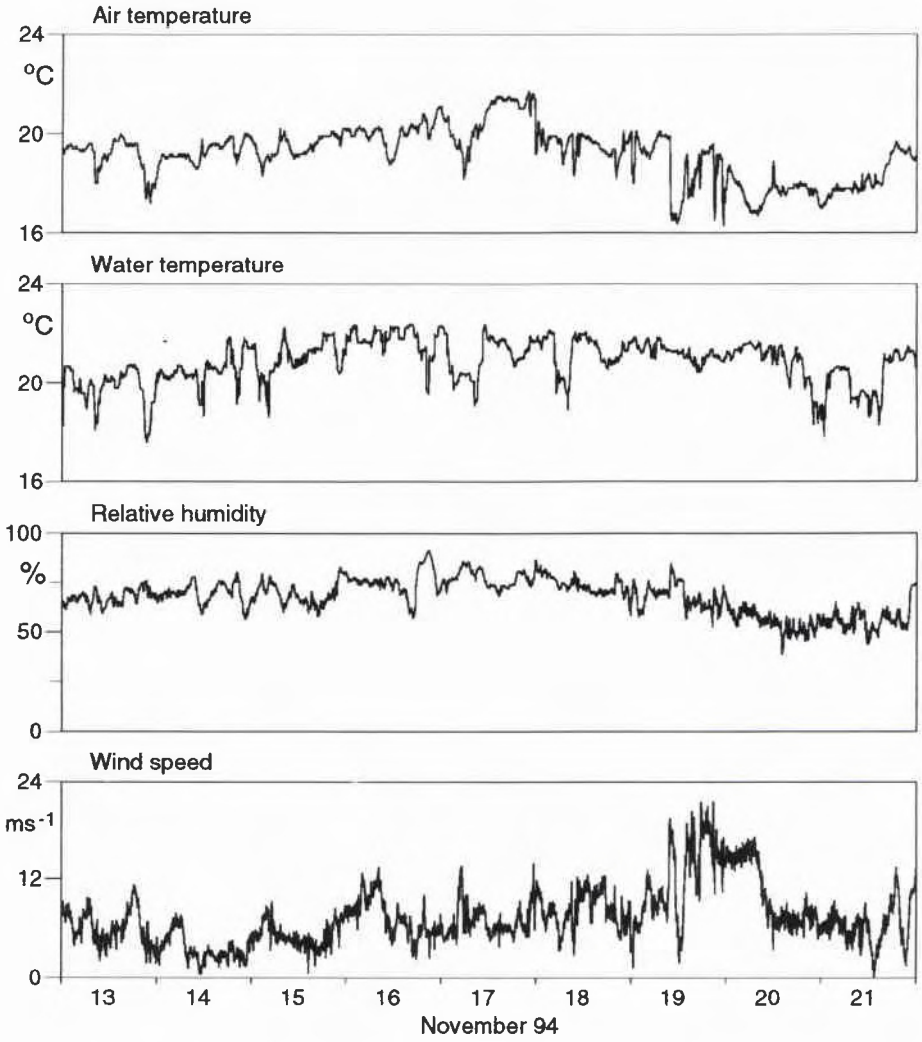

Figure B2: *Ship-borne measurements of air- and water temperature, relative humidity and wind speed during the Sicily-94 experiment.*

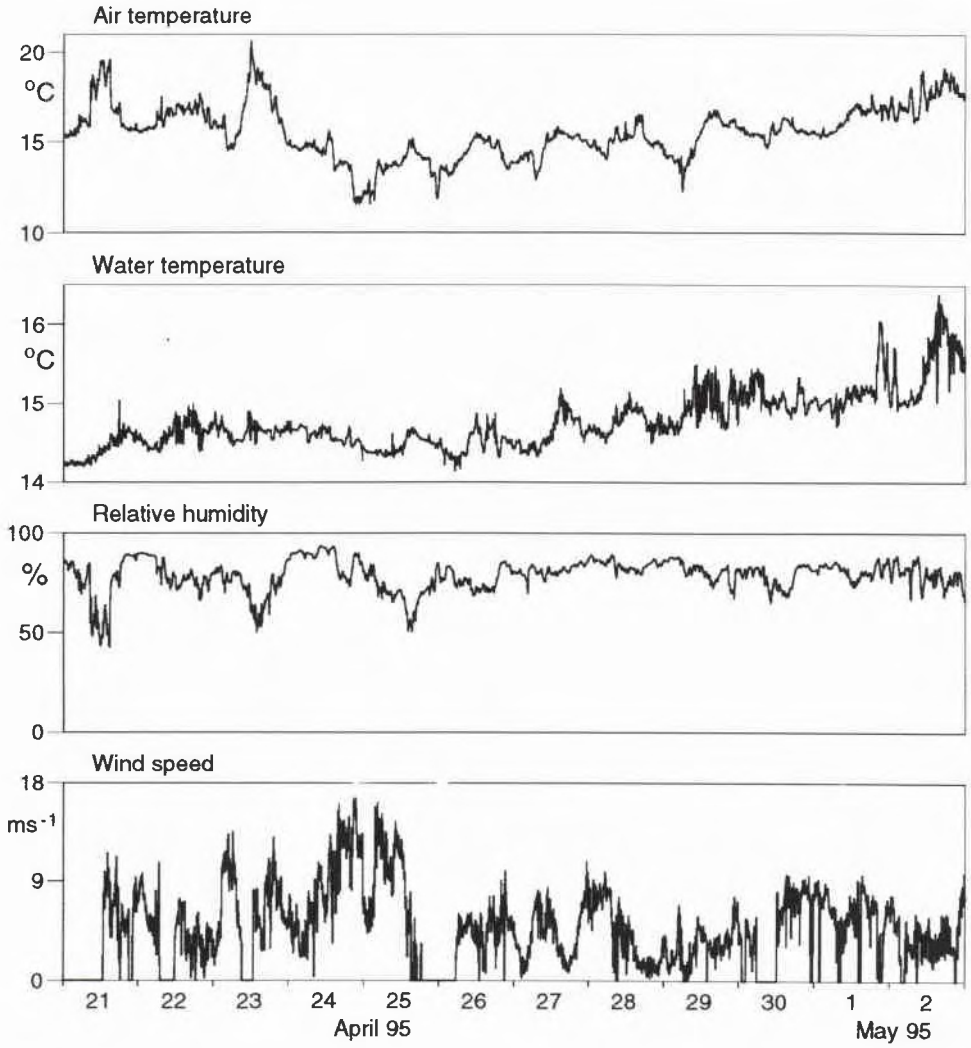

Figure B3: *Ship-borne measurements of air- and water-temperature, relative humidity and wind speed during the Elba-95 experiment.*

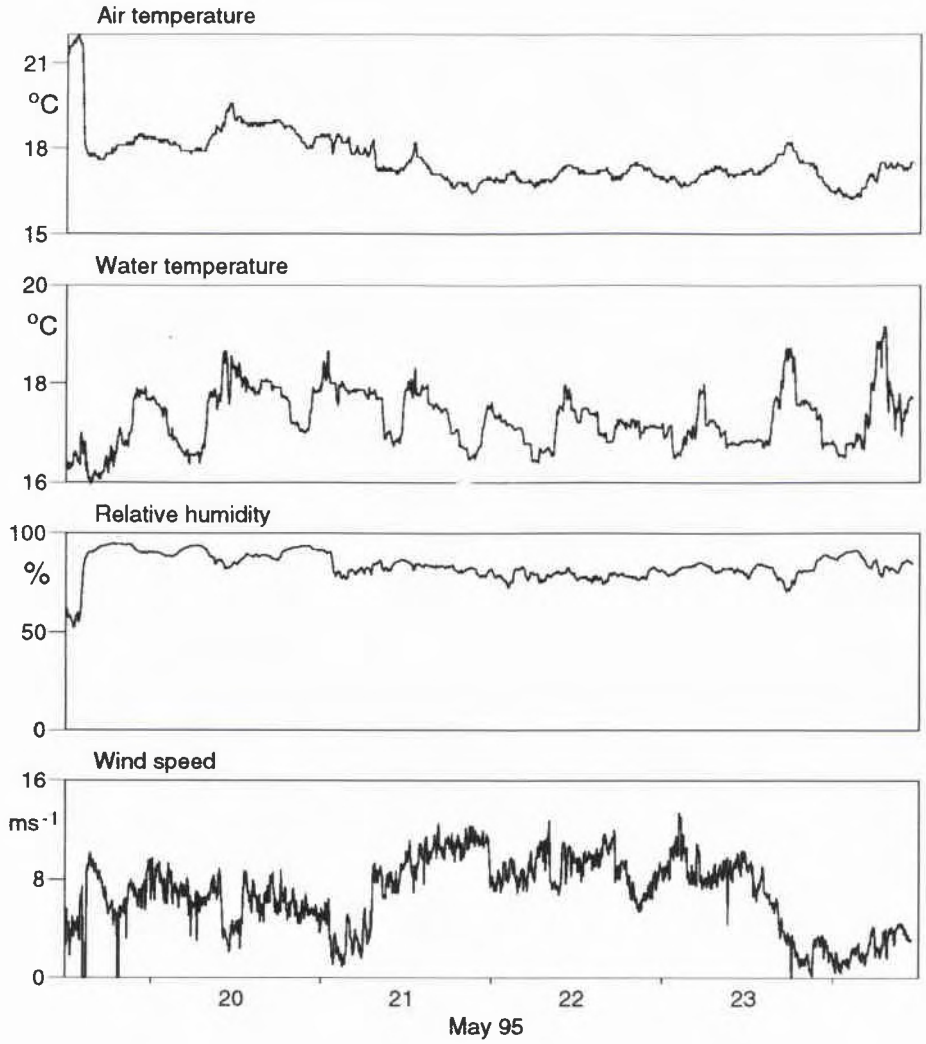

Figure B4: *Ship-borne measurements of air- and water-temperature, relative humidity and wind speed during the Otranto-95 experiment.*

Report no. changed (Mar 2006): SR-245-UU

Document Data Sheet

NATO UNCLASSIFIED

Security Classification		Project No.
NATO UNCLASSIFIED		23
Document Serial No.	**Date of Issue**	**Total Pages**
SR-245	January 1996	43pp.

Author(s)

H.-H. Essen

Title

On the predictability of subsurface sound speed from satellite-measured sea-surface temperature in the Mediterranean

Abstract

The report investigates the extent to which subsurface sound speed may be determined from satellite-measured sea-surface temperature (SST). Using CTD data from four hydrographic surveys in the Mediterranean, it is shown that the vertical sound-speed profiles can be decomposed into Empirical Orthogonal Eigenfunctions (EOF), with the first three functions accounting for at least 88% of the variance. Significant correlation between EOF amplitudes and SST has been found for only one of the three EOFs, either the 1st EOF or the 2nd EOF. In order to determine subsurface sound-speed from SST, this EOF has to represent important features of the sound-speed variability. This is the case for only one of the four surveys. Failures for the other surveys are due to a combination of low spatial variability of SST, not visible in the satellite-retrieved values, and complex vertical sound-speed profiles, which may not be represented by one EOF only.

Keywords

Mediterranean coastal waters – satellite imagery – sea-surface temperature – sound-speed profiles

Issuing Organization

North Atlantic Treaty Organization
SACLANT Undersea Research Centre
Viale San Bartolomeo 400, 19138 La Spezia, Italy

[From N. America: SACLANTCEN CMR-426 (New York) APO AE 09613]

Tel: +39 (0)187 540 111
Fax:+39 (0)187 524 600

E-mail: library@saclantc.nato.int

NATO UNCLASSIFIED

Report no. changed (Mar 2006): SR-245-UU

Initial Distribution for SR-245

Ministries of Defence	
DND Canada	10
CHOD Denmark	8
MOD Germany	15
HNDGS Greece	12
MARISTAT Italy	10
MOD (Navy) Netherlands	12
NDRE Norway	10
MOD Spain	2
MDN Portugal	5
TDKK Turkey	5
MOD UK	20
ONR US	49

NATO Authorities	
NAMILCOM	2
SACLANT	3
CINCEASTLANT/ COMNAVNORTHWEST	1
CINCIBERLANT	1
CINCWESTLANT	1
COMASWSTRIKFOR	1
COMMAIREASTLANT	1
COMSTRIKFLTANT	1
COMSUBACLANT	1
SACLANTREPEUR	1
SACEUR	2
CINCNORTHWEST	1
CINCSOUTH	1
COMEDCENT	1
COMMARAIRMED	1
COMNAVSOUTH	1
COMSTRIKFORSOUTH	1
COMSUBMED	1
SHAPE Technical Centre	1
PAT	1

SCNR for SACLANTCEN	
SCNR Belgium	1
SCNR Canada	1
SCNR Denmark	1
SCNR Germany	1
SCNR Greece	1
SCNR Italy	1
SCNR Netherlands	1
SCNR Norway	1
SCNR Portugal	1
SCNR Spain	1
SCNR Turkey	1
SCNR UK	1
SCNR US	2
SECGEN Rep. SCNR	1
NAMILCOM Rep. SCNR	1

National Liaison Officers	
NLO Canada	1
NLO Denmark	1
NLO Germany	1
NLO Italy	1
NLO Netherlands	1
NLO UK	1
NLO US	1

Total external distribution	205
SACLANTCEN Library	20
Total number of copies	225